R O W A N U N I V E R S I T Y

DIELECTRIC ELASTOMER ACTUATORS
- FINAL REPORT –

Phillip E. Thompson, Connor McLemore, James Rycek

I. ABSTRACT

The field of dielectric elastomer actuators is rapidly expanding. From artificial muscles to haptic feedback devices, these actuators are being researched as the solution to several problems in society today. It is the goal of this team to build upon previous research and expand this field of study at Rowan University. To that end, the team used the test apparatus created to test these actuators last semester, to characterize different polymers and additives. Simultaneously, the team worked to design new frame apparatuses to create minimum energy structures. Tests were run to determine the effects of additives and amount of applied voltage on actuation. Additionally, the team performed tensile tests to determine the effect the additives have on the material tensile strength.

The team successfully improved the existing test apparatus by obtaining a larger power supply and creating a program to ensure its safe use. The use of VHB tape as an actuator was repeated using the new experimental set-up. Two levels of pre-stretch were tested, 3 and 4. Larger pre-stretch and larger applied voltages led to larger amounts of actuation; the maximum strain achieved during this testing was 68% on a sample of VHB tape with a pre-stretch factor of 4. Silicone with 1 and 2 percent carbon black nanopowder by volume added were tested for both tensile strength and amount of actuation. 1% carbon black was found to have the best tensile strength, achieving an average stress of 13.9 MPa at an average stretch of 5. However, no actuation was seen during voltage testing up to 11 kV. For the future, more testing will have to be done to assess the use of this polymer for this application.

II. INTRODUCTION

A majority of the information on dielectric elastomers was obtained through a series of articles authored by Dr. Ronald Pelrine. Throughout these papers, Pelrine explains that dielectric elastomer actuators are a recently explored type of actuator which employs high voltage applied to a compliant, low modulus polymer acting as a dielectric. The attractive force between the cathode and anode of the capacitor-like setup causes a compressive force of the compliant dielectric. The setup is very similar to that of any normal capacitor. In the initial paper, published in 1998, Pelrine creates the mathematical model for actuation which is the standard accepted as the method of determining actuation force created by the electrical pressure on the system [1]. This formula is shown below in Equation 1.

$$P_{tot} = e_0 e_r \frac{U^2}{Z^2} \quad (1)$$

Where P_{tot} is the total force experienced by the elastomer, e_0 is vacuum permittivity, e_r is the dielectric constant of elastomer dielectric, U is the applied voltage and z is the distance between the cathode and anode (surfaces of the dielectric). Ignoring polarization of effective electric field

considerations, as defined by Nave [2] one can see that greatest force can be achieved by maximizing voltage, minimizing distance, minimizing modulus, and maximizing relative permittivity. In a following paper, Pelrine [3] and his fellow researcher presented data from several tests of varying elastomers, including several types of silicone rubbers, and VHB 4910, an elastomeric adhesive tape produced by 3M capable of 300% strains as described by 3M [4]. All had noticeable actuation strains in both linear and circular setups when exposed to appropriate high voltages. Listed dielectric strengths for VHB 4910 and Silicone Rubber limited applied voltages for available material thicknesses to less than 16 kV, as specified by 3M [4].

With the primary concepts of dielectric elastomers covered by the Pelrine papers, the next task undertaken was researching the optimization of these actuators for the future. One area of interest was the materials of construction; both the base polymer film used as well as chemical additives to the elastomers. These additives can be mixed into the base polymers during their curing to increase dielectric constants of the elastomers. Use of additives in previous experiments was met with mixed results as concluded by Nguyen [5]. Additives which lower modulus of elasticity and increase dielectric constant did improve actuation. However, trade-offs were noticed. While actuation at lower voltages became greater, voltage breakdown strength decreased. This limited the density of the electric field, and thereby lessened the actuation the dielectric elastomers could generate.

The second major area of research was minimum energy structures, described by Petralia [6]. These structures employ the use of normal dielectric elastomeric properties in conjunction with rigid-collapsible frames. Dielectric Elastomer Actuators are attached to these frames. Actuation force due to applied voltages combines with stored potential energy from the folded frames which hold the elastomers pre-stretched allow for actuation. The frames then act like spring elements, opposing the retracting forces of the elastomer wanting to return to their normal energy state, but the allowed collapsing of the frames allows for motions that could otherwise not be achieved with the completely rigid acrylic circle frames. An example of these structures is shown below in Figure 1.

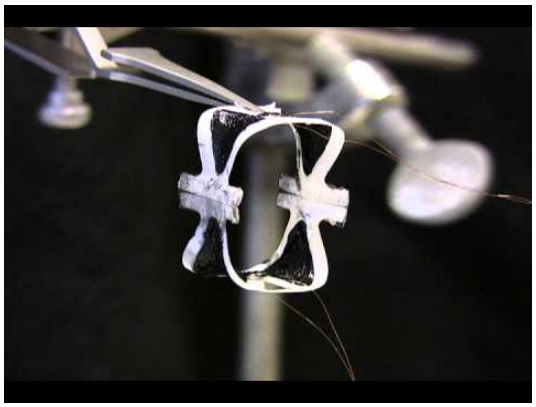

Figure 1: Folding Minimum Energy Structure

The goal of this project is to expand upon the foundational research on dielectric elastomer actuators at Rowan University. To accomplish this, the clinic team focused on addressing the shortcomings of the test apparatus developed last semester, especially the shortage of available voltage. The major goal was to use this improved test set-up to continue research on dielectric elastomer actuators by characterizing the existing polymers and the effects the additives have on their performance. It is hypothesized that the incorporation of the proper additives will increase the strain exhibited by the polymer samples. Secondly, the team will begin work on characterizing new minimum energy structure frames. It is further hypothesized that these new frames will provide greater and controlled actuation at lower applied voltages.

III. METHODOLOGY

Test Apparatus Modification

To test the elastomers at higher voltages, an EMCO high voltage power supply was obtained. This power supply required an input of 24 volts, and could output 0 to 33,000 volts. The power supply had no built-in interface, so a program in LabView was created to control the voltage output. The EMCO power supply was connected to the computer running the LabView program through a NI myDAQ data acquisition device. A circuit board with a built-in kill switch was made and wired in-between the power supply and the myDAQ so they could interface correctly. All wires were properly insulated and the circuit board was put in a plastic casing to minimize dangerous contact. The EMCO power supply, myDAQ, and circuit board were attached to an acrylic board to allow easy transportation and a safe set up. The power supply was also covered and surrounded in acrylic to prevent the user from accidently touching it and potentially being shocked.

Materials Research

To minimize the required applied voltage for these elastomer actuators, it is important to choose the correct materials of construction. Although this technology is still relatively new, a thorough literature review was done to determine what polymers and additives with which different researchers were having success. The field of base polymers used is very broad, but nearly all are urethanes or silicone-based. Because of this, the Dow Corning HS II RTV silicone polymer was used because it was readily available.

The list of potential additives was much longer and more specific. Certain chemicals respond much better to specific additives, so researchers are testing several types. The literature search lead to a final list of four potential additives to test in the coming years: carbon nanopowder, PMN-PT ceramic powder, titanium dioxide powder, and Rochelle salts. Rochelle salts are salt crystals that exhibit piezoelectric behavior. With this in mind, they were chosen as one of the two additives explored in the previous semester, making them readily available this semester. Thanks to a generous donation by the Cabot Corporation, a sample of Vulcan XC72R grade carbon black nanopowder was made available as the main additive for testing. Titanium dioxide was obtained a nearby department, making it an available choice for a third additive for testing. Ceramic powders have not yet been obtained , but are the first choice to expand the additive selection in the future.

In addition to the types of additives, the literature search was used to determine the amount of additive to add to the polymer films. This value happened to vary depending on the additive. For carbon nanopowder, the amount was in the range of 1-2% by volume. Therefore, samples of silicone polymer with both 1% and 2% carbon black were produced for testing. There were two major tests done to determine the effectiveness of the carbon black: a tensile test, and an actuation test.

The tensile test was done using the Shimpo machine. Small rectangular strips were cut from the cured polymer to be placed in the clamps of the machine. Tests were run to collect the amount of force at each level of displacement of the sample until failure. This data was then manipulated to obtain graphs of stress verses stretch of the sample, as well as breakdown points. The purpose was to determine not only how much stress these samples could withstand before failure, but also the optimum amount of pre-stretch for actuation testing. The data for silicone with additives was compared to both pure silicone and VHB tape.

Actuation Tests

The actuation testing was performed using the same test procedure developed last semester, but with the improved set-up. Circular samples of silicone with and without additives were fixed to rigid frames with electrodes attached. Voltage was then applied and pictures were taken at 1.1 kV increments. These pictures were used to measure the amount of actuation seen at each voltage. By measuring the diameter of the circle of conductive grease on the sample, the change in area of the sample could be determined. By comparing these values to the original area it was possible to display the area strain at each voltage as a percent change. As was done last semester, these tests were done with VHB to use as a control.

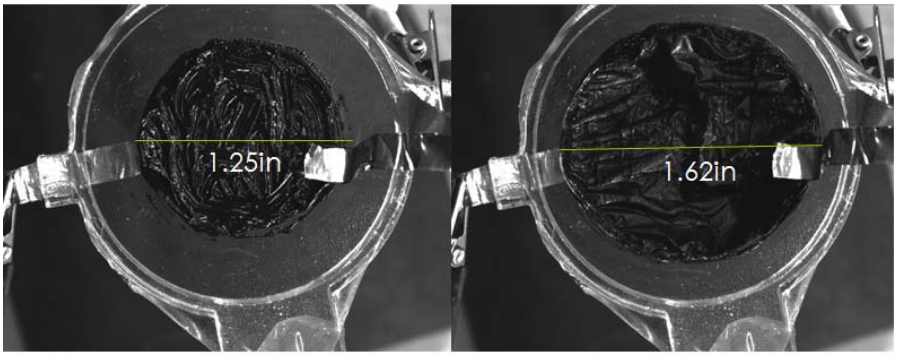

Figure 2: Actuation at 0 and 6.6 applied kV

Minimum Energy Structure Research

This semester, research areas of the Dielectric elastomer clinic were expanded. In the course of literature searches conducted in the early stages, several articles referencing devices called minimum energy structures were found. After further research, minimum energy structures were defined to be dielectric elastomers that employed compliant frames. The dielectric elastomer actuators require a certain level of biaxial pre-stretch to exhibit any significant levels of actuation. However, when attached to a rigid frame, the elastomer will only expand and contract within the confines of the frame. Minimum Energy Structures employ collapsible frames that

bend upon elastomer attachment and unbend when the elastomer actuates. The frames still hold the elastomer pre-tensioned, but can achieve a variety of different motions at theoretical lower voltages due to the presence of the spring element frame.

Relevant research into this field was conducted at MIT. According to the research by Petralia, using ABS plastic for collapsible frames, VHB tape and carbon conductive grease for compliant electrodes, small bending geometries were created that could actuate at as little as 1.2 kV.[6] These Dielectric Elastomer Minimum Energy Structures represented a large portion of early semester work dedicated to replicating and experimenting with their work and results. Several geometries were created, some based on Petralia's work and some simple geometries conducive to physical modeling. Some of these geometries created can be seen below in Figure 3.

Figure 3: Initial attempts at creating frames for specific types of motion

Several difficulties were encountered in the construction of these structures. Initial test samples produced zero visible actuation. It was determined that frame samples were too thick, and thus too ridged to produce actuation given the forces at play. Tests were repeated with a thinner grade of ABS film. At this point a separate problem was observed. The samples were experiencing breakdown or dielectric arcing prior to any visible actuation. While not confirmed, several hypothesized reasons for this was conductive grease forming conductive paths between either sides of the elastomer. Also, it was speculated that arcing at a certain voltage was occurring between the abs frames on either side of the elastomer. As a result, frames from that point were only applied to one side of the elastomer. A stable structure was finally achieve and tested. Minimal actuation was seen at 6kV. However, this actuation was extremely small and not easily quantifiable.

After reviewing literature searches, it was discovered that dielectric elastomers actuate at lower voltages with higher pre-strains, but actuate to much greater amounts in total with lower pre-strains.[8] At this point, testing was put on hold so the materials being used could be characterized on the Shimpo machine and the minimum energy structures could be mathematically modeled using solid mechanical analysis.

Currently, derivations for predicting the movement of DEMES are being calculated in Mathematica using principles of solid mechanics. The first derivation uses stress strain equation for each material used in the DEMES (elastomer and frame) at the initial and final states, with strain to the power of "n" to account for linear or nonlinear strain. This is shown in equation 2:

$$\sigma_1 = \epsilon_{i1}^{n} E_1 \tag{2}$$

Where stress is "σ", strain is "ϵ", and Modulus of Elasticity is "E". This is then integrated with respect to strain and volume to find both the initial and final total strain energies of the materials.

This is shown in equation 3:

$$U1i = \frac{V_1 \epsilon_{i1}^{1+n} E_1}{1+n} \tag{3}$$

Where "U" is the total strain energy of the material at the initial or final state and "V" is volume. The initial strain energies for the two materials are added together to find the total initial strain energy, and the final strain energies for the two materials are added together to find the total final strain energy. The initial and final strain energies are equal to each other because all energy is conserved in the system. This is shown in equation 4:

$$U1i + U2i == U1f + U2f \tag{4}$$

"U" is the total strain energy of the material at the initial or final state indicted by "i" for initial or "f" for final. At the final state the bonded materials are in equilibrium, so the sum of forces is equal to zero. This is shown in equation 5:

$$\Sigma F = E_1 * \epsilon_{f1} * A_1 + E_2 * A_2 * \epsilon_{f2} == 0 \tag{5}$$

Where "A" represents area and "F" represents force. The modulus of elasticity multiplied by the strain equals stress, and stress multiplied by an area equals a force, so the opposing forces create an equilibrium making the sum of forces zero. Because the initial and final energies are equal, and the initial strains are known for both materials, the final strains can be solved. Strain for one material is calculated through the equal initial and final total strain energies. This is shown in equation 6:

$$\epsilon_{f1} \to \left(\frac{(1+n)\left(\frac{V_1 \epsilon_{i1}^{1+n} E_1}{1+n} - \frac{V_2 \epsilon_{f2}^{1+n} E_2}{1+n} + \frac{V_2 \epsilon_{i2}^{1+n} E_2}{1+n} \right)}{V_1 E_1} \right)^{\frac{1}{1+n}} \tag{6}$$

The strain for the second material is calculated by finding the sum of final forces of both materials and equating it to zero. The sum of final forces equals zero because the bonded materials are at equilibrium. This is shown in equation 7:

$$\epsilon_{f2} \to -\frac{A_1 \epsilon_{f1} E_1}{A_2 E_2} \tag{7}$$

The two final strain equations are related, so to solve for them the strain of material 2 needs to be substituted into the equation for the strain of material 1. This will result in the value of the strain for material 1, which then can be used to calculate the strain of material 2. The second derivation was similar to the first; however, it took into account the height of the two materials (thickness) when calculating the total strain energy and also solved for the strain at the midpoint of where the strain for the top material and the strain for the bottom material met. It used equation 2 for the stress, but strain was set to the final strain minus the strain at the midpoint. This was divided by the height (thickness) of the material and multiplied by the height variable. This is shown in equation 8:

$$\epsilon_{i1} = \frac{z\,(\epsilon_{f1} - \epsilon_m)}{h_1} \tag{8}$$

Where "z" is the height variable, "ϵ_m" is the strain at the midpoint, and "h" is the height of the material. Similar to the first derivation, total strain energy of the material is found by integrating the strain equation with respect to strain, length width, and height. Height is integrated from 0 to "h1" for material 1, and 0 to "h2" for the second material. This is shown in equation 9:

$$U1 = L\,h_1\,w_1\,\epsilon_{f1}\,\epsilon_m + \frac{1}{4}\,L\,h_1\,w_1\,\epsilon_{f1}^2\,E_1 - \frac{1}{2}\,L\,h_1\,w_1\,\epsilon_{f1}\,\epsilon_m\,E_1 \tag{9}$$

In this equation, "n" is assumed to be 1 to make the strain linear. "L" is the length and "w" is the width. By adding together both total strain energies of the materials, the reference total strain energy is found. This is shown in equation 10:

$$Uref = U1 + U2 \tag{10}$$

To find the sum of forces at the final state, the equation 2 is multiplied by width and integrated with respect to height. This is done for both materials, which are then added together to find that the sum of forces equals zero. This is shown in equation 11:

$$F = h_1\,w_1\,\epsilon_{f1}\,E_1 + h_2\,w_2\,\epsilon_{f2}\,E_2 = 0 \tag{11}$$

Equation 11 can be used to find the final strain of material 1, shown here in equation 12:

$$\epsilon_{f1} \to -\frac{h_2\,w_2\,\epsilon_{f2}\,E_2}{h_1\,w_1\,E_1} \tag{12}$$

The strain of material 2 is found by setting equation 10 and equation 11 equal to each other, and is shown here in equation 13:

$$\epsilon_{f2} \to \frac{4\left(\epsilon_m - \epsilon_m\,E_2 + \frac{\epsilon_m\,E_2}{E_1}\right)}{-E_2 + \frac{h_2\,w_2\,E_2^2}{h_1\,w_1\,E_1}} \tag{13}$$

Similar to the first derivation, by substituting the final strains into their related equations, the values of the final strains can be calculated. The strain at the midpoint is found by taking a partial derivative equation 10 with respect to the strain at the midpoint "$\in_m$". This is shown in equation 14:

$$\epsilon_m = -L\,h_2\,w_2\,\epsilon_{f2} + L\,h_2\,w_2\,\epsilon_{f2}\,E_2 - \frac{L\,h_2\,w_2\,\epsilon_{f2}\,E_2}{E_1} \tag{14}$$

The third derivation solves for the midpoint of height with respect to strain of the materials when they are bonded together, and solves for the final maximum strain of both materials which would be at the very top and very bottom of the bonded materials. The stress (equation 2) was integrated with respect to strain for both materials at both the initial states. The final strain of material 1 was then set equal to a negative height variable "-y" divided by the thickness of the material "C_1" and multiplied by the max strain of material 1. This is shown in equation 15:

$$\epsilon_{f1} = \frac{-y}{C_1}\,\epsilon_{max1} \tag{15}$$

The final strain of material 2 was then set equal to a negative height variable "-y" divided by the thickness of the material "C_2" and multiplied by the max strain of material 2. This is shown in equation 16:

$$\epsilon_{f2} = \frac{-y}{C_2}\,\epsilon_{max2} \tag{16}$$

The initial states are then integrated again with respect to width, length, height and strain to find the initial total strain energy. This is shown in equation 17:

$$U_{i1} = \frac{1}{2}\,t_{i1}\,(C_1 - y_m)\,\Delta x_{i1}\,\epsilon_{max1}^2\,E_1 \tag{17}$$

Where "t" is width and "Δx" is length. The final states are integrated with respect to strain, length, width, and height going from the unknown middle of the material "y_m" to the known heights of the materials "C_1" and "C_2" to find the total strain energies of the two materials. This is shown in equation 18:

$$U_{f1} = \frac{1}{6}\,C_1\,t_{f1}\,\Delta x_{f1}\,\epsilon_{max1}^2\,E_1 - \frac{t_{f1}\,y_m^3\,\Delta x_{f1}\,\epsilon_{max1}^2\,E_1}{6\,C_1^2} \tag{18}$$

The maximum strains of the materials at the final state are then found by solving for them by setting the initial and final total strain equal to each other and by setting the sum of forces at the final state to zero. These strains are shown in the following equations 19 and 20:

$$\epsilon_{max1} \to \frac{\sqrt{\frac{1}{6} C_2 t_{f2} \Delta x_{f2} \epsilon_{max2}^2 E_2 + \frac{t_{f2} y_m^3 \Delta x_{f2} \epsilon_{max2}^2 E_2}{6 C_2^2} - \frac{1}{2} t_{i2} (C_2 + y_m) \Delta x_{i2} \epsilon_{max2}^2 E_2}}{\sqrt{-\frac{1}{6} C_1 t_{f1} \Delta x_{f1} E_1 + \frac{t_{f1} y_m^3 \Delta x_{f1} E_1}{6 C_1^2} + \frac{1}{2} t_{i1} (C_1 - y_m) \Delta x_{i1} E_1}} \tag{19}$$

$$\epsilon_{max2} \to \frac{C_2 \left(C_1^2 \epsilon_{max1} E_1 - y_m^2 \epsilon_{max1} E_1\right)}{C_1 \left(C_2^2 - y_m^2\right) E_2} \tag{20}$$

The midpoint height with respect to the final strain energy of the bonded material is found by taking a partial derivate of the final total strain energy with respect to "y_m", the unknown midpoint. This is shown in equation 21:

$$y_m = -\frac{t_{f1} y_m^2 \Delta x_{f1} \epsilon_{max1}^2 E_1}{2 C_1^2} + \frac{t_{f2} y_m^2 \Delta x_{f2} \epsilon_{max2}^2 E_2}{2 C_2^2} \tag{21}$$

Future calculations will predict the bending angle of the bonded materials, which will be useful in choosing the strains and dimensions of DEMES test structures.

IV. RESULTS

Silicone samples with 1 and 2 percent carbon black by volume were tested to determine the additive's effect on the elastic properties of the base silicone. Three samples of each additive percentage were tested, along with three samples of pure silicone to use as a control. Two samples of VHB were also tested in attempt to further understand the material. Figure 4 shows the levels of stretch and stress that each sample achieved before failure.

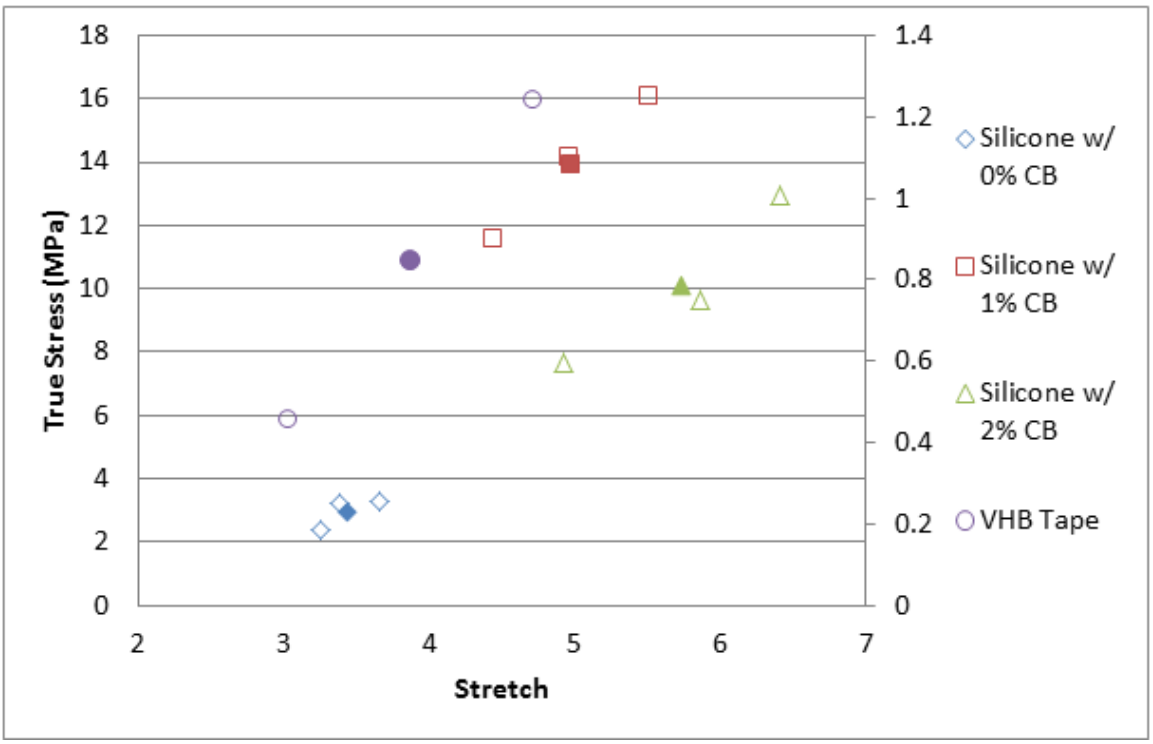

Figure 4: Stress on each material as a function of the observed stretch.

Because the properties of VHB tape are so different than those of the silicone, those trials are plotted along a different y-axis, denoted by the arrows (although both axes show true stress). The repetitions are all found to be fairly precise in their grouping, particularly the pure silicone samples. Strictly from a mechanical standpoint, 1% carbon black by volume is the better amount of additive to use to move on for actuation testing. This is because the samples overall could withstand the largest stresses while still obtaining large stretches before failing. It is worth noting however, that the pure silicone samples were much older than the samples with additives, which could have had effects on the elasticity of the samples. To ensure accuracy in these findings, this testing should be repeated again.

Knowing the best sample to use from a breakdown standpoint, the entire graph of each sample was examined to determine what amount of stress was optimal for the sample. When looking at a graph of stress vs stretch, the optimal point to look for is a region when the sample undergoes the largest change in stretch at the lowest change in stress. These curves for each sample tested are shown in Figure 5.

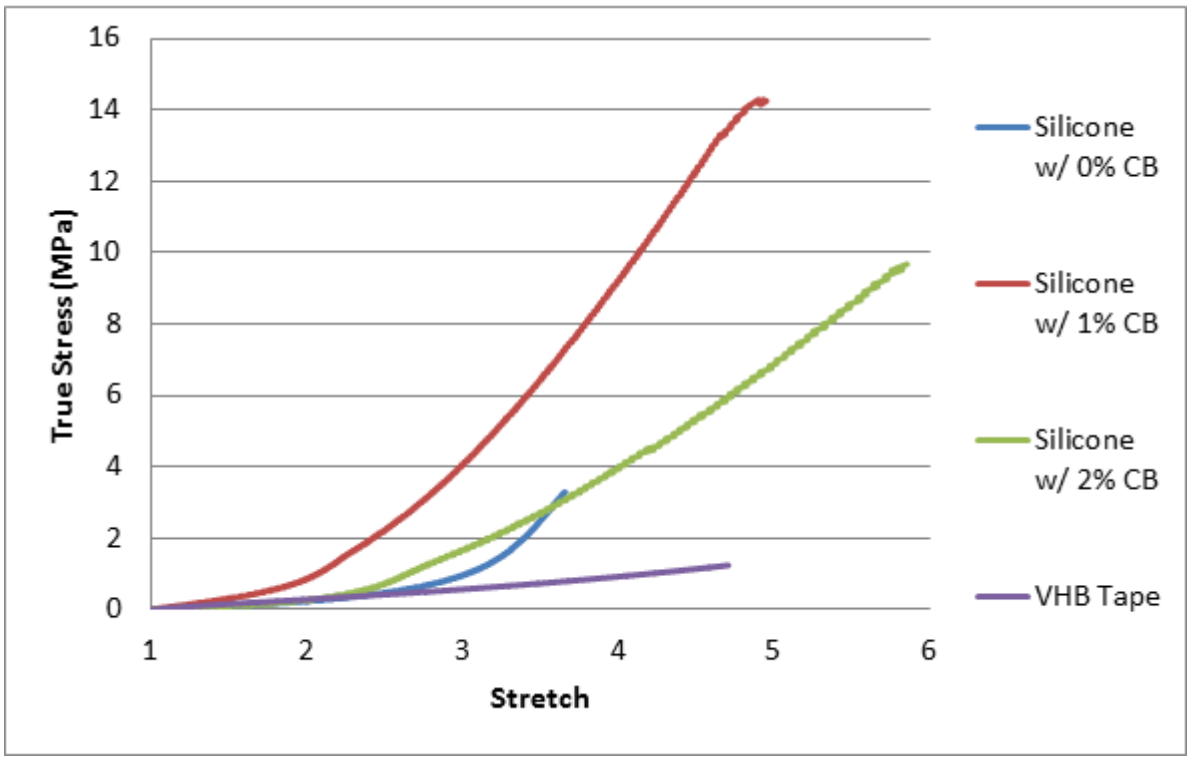

Figure 5: Stress vs stretch graph for each material, generated from tensile testing data

As seen in the graph, all samples start out very flat, changing in stretch without much change in stress. After a stretch of about 2 the slope of the line for all silicone samples begins increasing significantly, correlating to a greater increase in stress to obtain a smaller change in stretch. The VHB is shown to be able to stretch with seemingly no issue, leading to the incredible amounts of strain the material can exhibit. These results show that these silicones should not be stretched much more than 200% uni-axially, which allows much smaller area strains.

Using the improved set-up, the team was able to recreate the use of VHB as a viable polymer actuator. For two different levels of pre-stretch (3 & 4), significant actuation was exhibited with as little as 1100 kV of applied voltage. Figure 6 below shows the level of strain achieved at each increment of applied voltage.

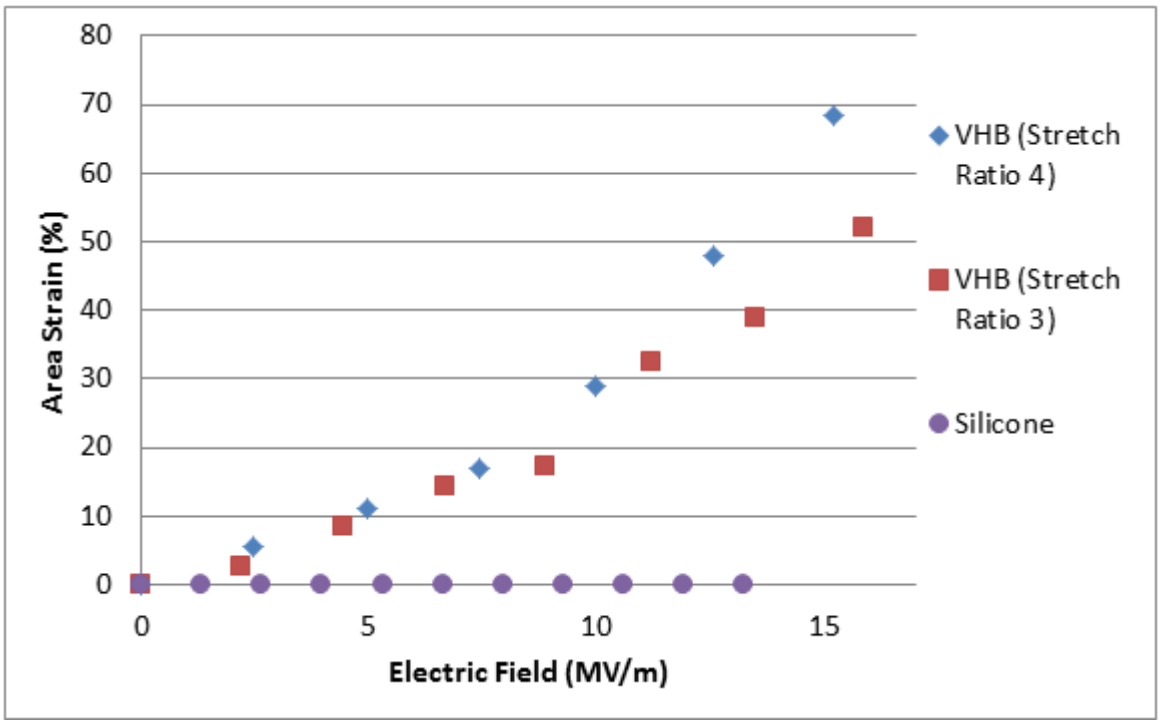

Figure 6: Actuation shown by each material as a function of applied electric field

To simplify the graph, all silicone samples were grouped together because they exhibited no actuation. Electric field correlates directly to the applied voltage, but takes the sample thickness into account, which is always changing during actuation testing. A larger amount of biaxial pre-stretch causes minimized thickness, which explains why the sample of VHB with a larger stretch is shown to withstand a greater electric field at the same voltage. For VHB, it is shown that an increase in stretch factor correlates to larger actuations, but only when larger electric fields are applied. In an electric field less than approximately 8 MV/m, both VHB samples showed very similar amounts of actuation. After this point, the sample of VHB with the stretch ratio of 4 began to show much greater actuation at the same applied field. These results show that larger amounts of pre-stretch correlate to larger observed actuations, but only at the higher electrical fields.

V. CONCLUSIONS

Significant progress was made in improving the test set-up for actuation testing. The larger power supply was successfully installed and housed, which will make a larger variety of testing possible for the future. Progress was also made in researching the new minimum energy structure frames. Mathematica codes were successfully programmed to further understand the forces and bend angles involved in these structures. This program will make it easier to design new frames in the future.

As for the material research, the results are more mixed. Good progress was made in identifying possible materials and testing the validity of their use for these applications. While the current silicone samples are capable of exhibiting large strains just as the VHB tape does, they simply require larger applied pressures to make these strains. Because these pressures directly correlate to the applied voltage, these silicone samples will require much more voltage to actuate. The current silicone samples also cannot exhibit very high levels of pre-stretch without leading to detriments from the stress felt. Unfortunately, this may render this particular combination of silicone and carbon black useless for these applications. In the future more testing should be done to determine if any actuation can be obtained from the Dow Corning HS II RTV silicone with carbon black. If not, focus will have to be shifted to different polymers and/or additives.

References:

1. R. Pelrine and R. Kornbluh. “Electrostriction of polymer dielectrics with compliant electrodes as a means of actuation”. SRI International, 333 Ravenwood Ave., Menlo Park, CA. 1998

2. R. Nave. “Polarization of Dielectric”. Internet: http://hyperphysics.phy-astr.gsu.edu/hbase/electric/dielec.html. Accessed 2012

3. R. Pelrine and R. Kornbluh. “High-field deformation of elastomeric dielectrics for actuators”. SRI International, 333 Ravenwood Ave, Menlo Park, CA . 1999

4. 3M VHB Tape Technical data. Dielectric Strength for VHB 4910. 2011

5. H.C. Nguyen and V.T. Doan. “The effects of additives on the actuating performances of a dielectric elastomer actuator”. School of Mechanical Engineering, Sungkyunkwan University, Chunchon-dong 300, Jangan-gu, Suwon, 440-746, Korea. 2009

6. M.T. Petralia and R.J. Wood. “Fabrication and analysis of dielectric-elastomer minimum-energy
structures for highly-deformable soft robotic systems”. The 2010 IEEE/RSJ International Conference on Intelligent Robots and Systems. Taipei, Taiwan. 2010

7. Innovative Polymers RTV Silicone Rubber Physical Properties. Dielectric Strength. 2009

8. T, Lu et al. “Dielectric elastomer actuators under equal-biaxial forces, uniaxial forces, and uniaxial constraint of stiff fibers.” Soft Matter. [Online]. Vol. 8, pp. 6167-6173. Available:http://pubs.rsc.org/en/content/articlehtml/2012/sm/c2sm25692d, Accessed 2013.